Available online at www.sciencedirect.com

SciVerse ScienceDirect

Ceramics International 38 (2012) 1093–1098

CERAMICS INTERNATIONAL

www.elsevier.com/locate/ceramint

Influence of in-situ magnetic field pressing on the structural and multiferroic behaviour of $BiFeO_3$ ceramics

T. Karthik [a,1], A. Srinivas [b,*], V. Kamaraj [a], V. Chandrasekeran [b]

[a] Department of Ceramic Technology, A.C.Tech Campus, Anna University, Chennai 600025, Tamil Nadu, India
[b] Advanced Magnetics Group, Defence Metallurgical Research Laboratory, Hyderabad 500058, Andhra Pradesh, India

Received 16 March 2011; accepted 19 August 2011
Available online 26 August 2011

Abstract

Polycrystalline single phase $BiFeO_3$ (BFO) ceramic samples have been prepared by conventional solid state sintering and also by in-situ magnetic field pressing followed by solid state sintering. The influence of in-situ magnetic field pressing on the structural, magnetic, ferroelectric and thermal properties has been investigated in this work. X-ray diffraction analysis and Reitveld refinement shows the single phase characteristics of BFO samples. Further texture formation and the development of compressive lattice strain have been observed in the magnetic field pressed samples. A change in Fe–O–Fe bond angle and suppression of spiral spin structure results in the enhanced magnetization value M_s = 136 memu/g at 2 T. Similarly spontaneous polarization has also improved with a P_{max} value of 1.3 μC/cm^2. DSC plot shows a significant variation in heat flow and enthalpy at the Neel transition (T_N = 372 °C) and ferro to paraelectric transition (T_C = 820 °C) for the magnetic field pressed BFO samples.

Keywords: A. Sintering; B. X-ray Methods; C. Ferroelectric properties; C. Magnetic properties

1. Introduction

There has been increasing interest in multiferroics, which are materials that show spontaneous magnetic and electric ordering in the same phase. The coupling between these magnetic and electric degrees of freedom gives rise to potential applications in Spintronic devices and Sensors [1,2]. $BiFeO_3$ is the most interesting material in the family of a very few single phase multiferroics because of its high phase transition temperature, i.e., Curie transition temperature $T_C \sim 1103$ K and antiferromagnetic Neel transition temperature $T_N \sim 643$ K [3]. Since its discovery, the practical applications of this material have been hampered due to its large current leakage and difficulty in synthesizing single phase $BiFeO_3$. Several techniques such as solid state reaction, sol–gel synthesis, hydrothermal synthesis, high energy ball milling, and rapid liquid phase sintering have been successful in synthesizing of pure $BiFeO_3$ [4,5]. Bulk BFO especially synthesized through solid solution, exhibits weak ferromagnetic properties at room temperature due to residual moment from a canted spin structure, which is generated from the impurity phases related to Fe phase separation [6]. There are several reports on the processing of BFO dispersed in $BaTiO_3$ matrix to restrict the second phase, leakage current and low resistivity in the sample [7]. Recently it has been shown that rapid liquid phase sintering of $BiFeO_3$ can result in a high resistivity and polarization value of $BiFeO_3$, but can also lead to high dielectric loss and more defects [8]. In our recent work, improved magnetoelectric output was observed in the $BaTiO_3$–$BaFe_{12}O_{19}$ composite system by using in-situ magnetic field pressing [9]. Hence the effect of magnetic field during pressing on the magnetic and ferroelectric properties is also inevitable. In this present work, one set of samples of $BiFeO_3$ ceramic was prepared by conventional solid state sintering. Another set of samples were prepared by subjecting them to in-situ magnetic field pressing followed by solid state sintering.

2. Experimental details

Samples of $BiFeO_3$ ceramics were prepared by using high purity Bi_2O_3 and Fe_2O_3 (99.99% Sigma Aldrich Chemicals,

* Corresponding author. Tel.: +91 40 24586835; fax: +91 40 24340884.
E-mail addresses: adirajs@dmrl.drdo.in, adirajs@yahoo.com (A. Srinivas).
[1] Present address: Department of Materials Science and Engineering, Indian Institute of Technology Hyderabad, ODF Campus, Yeddumailaram, Andhra Pradesh 502250, India.

0272-8842/$36.00
doi:10.1016/j.ceramint.2011.08.036

USA). The precursors were weighed according to mol% calculations and milled for 2 h using toluene as a medium. The samples were pre-calcined at 700 °C for 1 h. The calcined powders were pressed into pellets using uniaxial hydraulic press and another set of powders were pressed into pellets by using in-situ magnetic field press with an applied magnetic field of 1 T along the axial direction. The schematic diagram of in-situ magnetic field press was given in our previous work [9]. Stainless steel die of 12.5 mm diameter with a Tungsten carbide inner lining was used for the compaction of pre-calcined powders. A load of 100 bar was applied vertically from the bottom. These pellets were sintered in air atmosphere at 820 °C for 2 h with a heating rate of 5 °C per min. X-ray diffraction analysis of the sintered pellets were performed using Philips X-ray diffractometer PW-1320 at 2θ scan rate of 0.1 degree per minute with CuKα incident radiation. Magnetization measurements were performed using vibrating sample magnetometer (ADE systems, Model no-EV9, USA). The sintered discs were polished, coated with silver paste and annealed at 300 °C for 30 min for ferroelectric measurements using automatic P vs. E loop tracer. High temperature DSC measurements were carried out using TA instruments.

3. Results and discussions

Fig. 1(a) shows the XRD patterns of single phase $BiFeO_3$ ceramic prepared by conventional solid state sintering (BFO-CS) and by in-situ magnetic field pressing followed by solid

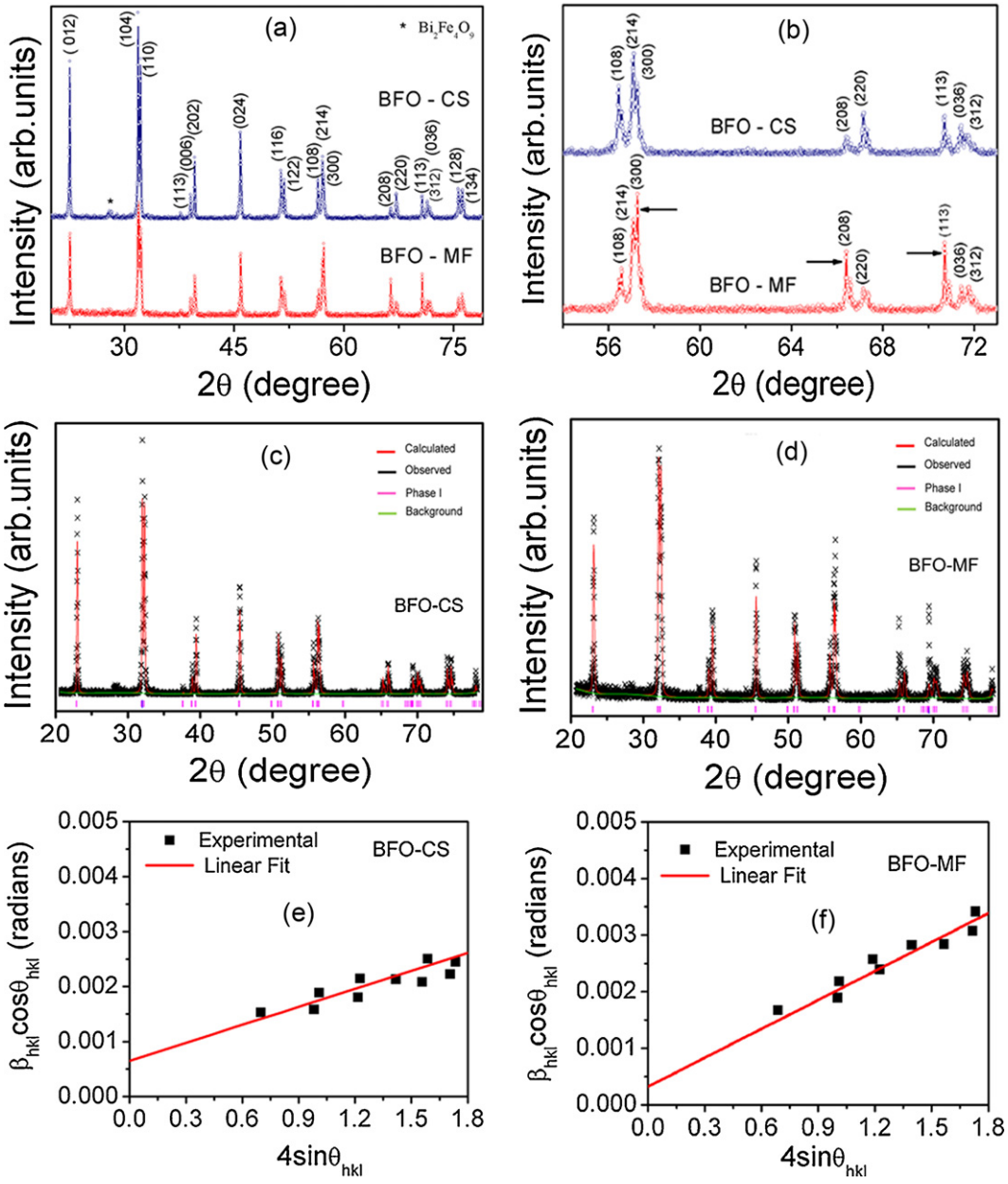

Fig. 1. (a) X-ray diffraction patterns of conventionally sintered (BFO-CS), in-situ magnetic field pressed and sintered $BiFeO_3$ samples (BFO-MF); (b) texture formation in BFO-MF sample (as indicated by arrows); Reitveld analysis of (c) BFO-CS and (d) BFO-MF samples (the allowed Bragg reflections for the corresponding R3c space group is indicated by ticks), W–H plot of (e) BFO-CS and (f) BFO-MF samples.

state sintering (BFO-MF) respectively. It was observed that the ceramics processed by both routes have single phase characteristics with $BiFeO_3$ as a major phase and a trace amount of $Bi_2Fe_4O_9$ as secondary phase has formed, which is unavoidable during the kinetics of formation of $BiFeO_3$. In the magnetic field pressed samples, a decrease in the intensity of Bragg reflections from major planes was observed when compared to the conventionally processed BFO ceramics. On close observation of the XRD patterns as shown in Fig. 1(b) a significant increase in the intensity of the Bragg reflections respectively from (3 0 0), (2 0 8) and (1 1 3) planes, were observed in the in-situ magnetic field pressed BFO ceramic as indicated by arrows. This observed increase in intensity of the Bragg reflections indicates that there is a texture formation in the magnetic field pressed samples. Since $BiFeO_3$ belongs to the rhombohedral crystal system, it has higher anisotropy nature than the cubic crystal system. Hence the magnetic field applied during pressing induces anisotropy in terms of texture formation in the magnetic field pressed samples.

Reitveld analysis was performed as shown in Fig. 1(c) and (d) using the DISAGL version win 32, crystal structure, distance and angle program. The Reitveld refined lattice parameter of conventionally processed BFO ceramic shows a_{hex} = 5.5843 Å, c_{hex} = 13.8817 Å, V (Å^3) = 374.905 (χ^2 = 1.485). The magnetic field pressed sample exhibits a lattice parameter of a_{hex} = 5.5810 Å, c_{hex} = 13.8748 Å with a reduced unit cell volume V (Å^3) = 374.270 (χ^2 = 1.575). From the refinement it shows that R3c symmetry was retained in both the samples. Similar to the reduction in unit cell volume, the magnetic field applied during compaction also induces a change in the Fe–O–Fe bond angle as tabulated in Table 1. Further the reduced *c/a* ratio values, unit cell volume and the change in the Fe–O–Fe bond angle of about 0.6° in the magnetic field pressed BFO sample shows that the magnetic field applied axially during compaction, induces some compressive strain on the crystal lattice. It is well known that Goldschmidt proposed a tolerance factor to quantify the size match of the A and B cations to the cubic perovskite topology [10]. The tolerance factor, τ is defined as $\tau = (r_A + r_B)/[2^{1/2}(r_B + r_O)]$ in ABO_3 perovskites. r_A, r_B and r_O are the ionic radii of A in 12-fold coordination, B in 6-fold coordination and O in 6-fold coordination, respectively. When the tolerance factor is less than unity, the B–O bonds are compression and the A–O bonds are under tension [11]. In $BiFeO_3$ the tolerance factor is less than unity, hence the oxygen octahedral must buckle in order fit into a cell that is too small. For $BiFeO_3$, ω is ca. 11–14° around the polar [1 1 1] axis which is directly related to the Fe–O–Fe angle. Hence it leads to a lattice strain associated with the crystal system. Further during high temperature sintering followed by cooling results in the formation of strain due to thermal stresses. The contribution of these lattice strains throughout the microstructure is often denoted as micro strain. The modified physical properties of materials are mostly attributed to the very large percentage of interfacial region with a modified microstructure. However recent experiments have concluded that the lattice strain in samples also significantly contributes to the modified physical properties. The mean magnitude of the local strains in samples could be estimated from the X-ray diffraction pattern using different analytical procedures. The lattice strain in $BiFeO_3$ ceramic was estimated using the Williamson–Hall relation [12,13]. In Williamson–Hall method it is assumed that the line broadening β_t of a Bragg reflection ($h\,k\,l$) originates from small crystallite size and follows Scherrer's equation $\beta_t = K\lambda/t\cos\theta_{h\,k\,l}$. Here K is the shape factor, λ is the X-ray wavelength of X-ray beam, $\theta_{h\,k\,l}$ is the Bragg angle and t is the effective crystallite size normal to the reflecting planes. Instrumental contribution to line broadening of the diffraction pattern was recorded using standard silicon and their corresponding full width half maximum was measured. The instrumental corrected broadening ($\beta_{h\,k\,l}$) corresponding to each diffraction peak of $BiFeO_3$ was estimated using the relation

$$\beta_{hkl} = \left[(\beta_{hkl})^2_{\text{measured}} - \beta^2_{\text{measured}}\right]^{0.5} \quad (1)$$

Also the strain induced broadening β_ε is given by the Wilsons formula as $\beta_\varepsilon = 4\varepsilon\tan\theta_{h\,k\,l}$. Here ε is the root mean square value of the microstrain. Assuming that the particle size and strain contributions to the line broadening are independent of each other and both have a Cauchy like profile, the observed line breadth is then, simply sum of the two, i.e.,

$$\begin{aligned}\beta_{hkl} &= \beta_t + \beta_e = [K\lambda/t\cos\theta_{hkl}] + [4\varepsilon\tan\theta_{hkl}]\\ \beta_{hkl}\cos\theta_{hkl} &= [K\lambda/t] + [4\varepsilon\sin\theta_{hkl}]\end{aligned} \quad (2)$$

Eq. (2) is the William–Hall equation. The values of $\beta_{h\,k\,l}\cos\theta_{h\,k\,l}$ as a function of $4\varepsilon\sin\theta_{h\,k\,l}$ was plotted and the microstrain ε can be estimated from the slope of the line as shown in Fig. 1(e) and (f). The values of $\beta_{h\,k\,l}$ used here is the instrumental corrected values. The lattice strain for BFO-CS sample was estimated as 0.00109. Similarly the micro strain for the in-situ magnetic field pressed and sintered $BiFeO_3$ (BFO-MF) was found to be 0.00170. It shows that the magnetic field pressed samples shows higher strain values than their counterpart. This increased strain value corresponds to the influence of the magnetic field during pressing on the crystal lattice. Further the higher degree shift in 2θ position

Table 1
Reitveld refined lattice parameters and Fe–O–Fe bond angle for conventional and magnetic field pressed BFO ceramics.

Sample	Lattice parameters	Space group	*c/a* ratio	Volume (Å^3)	Bond angle $\theta_{Fe-O-Fe}$
BFO-CS	a_{hex} = 5.5843 Å c_{hex} = 13.8817 Å	R3c	2.4858	374.884	155.668
BFO-MF	a_{hex} = 5.5810 Å c_{hex} = 13.8748 Å	R3c	2.4860	374.225	155.053

Table 2
Difference in 2θ position values corresponding to the major Bragg reflections from conventional and magnetic field pressed BFO ceramic samples.

Sample	2θ position corresponding to the Bragg reflections from planes			
	(0 1 2)	(1 0 4)	(1 1 0)	(2 0 4)
BFO-CS	22.388	31.709	32.029	45.692
BFO-MF	22.402	31.727	32.049	45.720

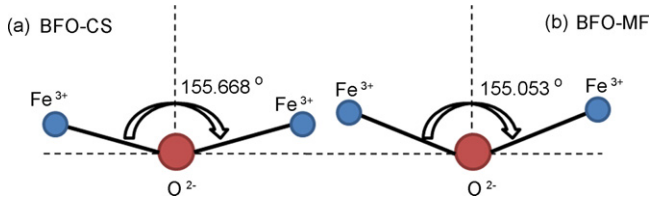

Fig. 3. Change in Fe–O–Fe bond angle in $BiFeO_3$ ceramics due to the influence of magnetic field pressing.

corresponding to the major Bragg reflections of magnetic field pressed samples as tabulated in Table 2 also confirm that there is a compressive strain persists in the system.

Room temperature magnetic hysteresis loops for both the samples exhibits a weak ferromagnetic loop with non-zero coercivity and remanence values as shown in Fig. 2(a). The conventionally sintered BFO ceramics exhibits a magnetization value of $M_s = 106$ memu/g and the magnetic field pressed sample shows enhanced magnetization value of $M_s = 136$ memu/g. In the magnetic field pressed samples, a significant increase in saturation magnetization (M_s) is attributed to the suppression of spiral spin structure and change in the Fe–O–Fe canting angle [14]. In $BiFeO_3$ the spins

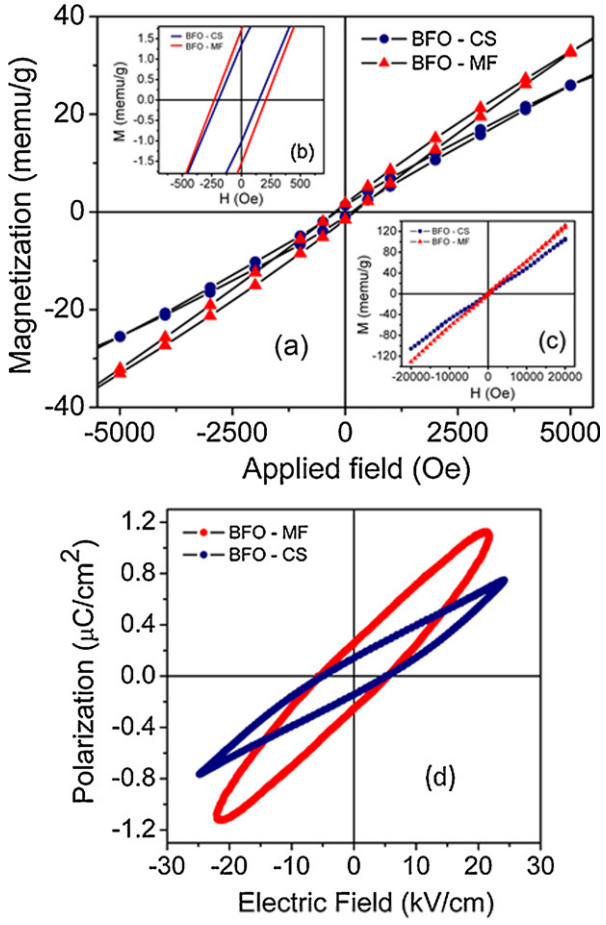

Fig. 2. (a) M–H plots of BFO-CS and BFO-MF samples up to 5.5 kOe. The inset (b) shows the M–H loops up to 500 Oe and (c) shows M–H loops up to 2 T, (d) ferroelectric (P–E) loops for conventional and magnetic field pressed $BiFeO_3$ samples.

of the two sublattices are not quite antiparallel but have a canted spin structure. Hence the interaction between the two Fe^{3+} ions (high spin configuration) through O^{2-} ion, i.e., Fe^{3+}–O^{2-}–Fe^{3+} exchange interaction results in net magnetic moment. This Fe–O–Fe bond angle in $BiFeO_3$ controls both the magnetic exchange and orbital overlap between Fe and O; hence a change in this bond angle as shown in Fig. 3 is responsible for the improved magnetic ordering in BFO. Further it was reported that a very high magnetic field of 18 T could even destroy the modulated spiral spin structure [15]. The magnetic field applied during in-situ magnetic field pressing was only 1 T; hence it cannot completely suppress the spiral spin structure. Thus only a small change was observed in the magnetization values. The remanent magnetization M_r was found to be 1.36 memu/g for BFO-CS and the magnetic field pressed BFO ceramics exhibits $M_r = 1.68$ memu/g. A small increase in M_r value in the BFO-MF samples is due to the suppression of the space modulated spin structure. Similar to the magnetization values, a non-zero coercive field values for both the samples are observed as shown in the inset (b) of Fig. 2. The non-zero coercivity values indicate that a weak ferromagnetism persists in the BFO ceramics. This origin of weak ferromagnetism in BFO ceramics processed by both the techniques are primarily due to the distribution of Fe^{2+} and Fe^{3+} ions created due to charge compensation and their magnetic interaction between them leads to spontaneous magnetization [16].

The ferroelectric hysteresis loops measured at room temperature was shown in Fig. 2(d). The spontaneous polarization (P_{max}), remanent polarization (P_r), and the coercive field (E_c) are about 0.75 μC/cm^2, 0.3 μC/cm^2, and 5 kV/cm respectively for the conventionally sintered BFO ceramics. In the magnetic field pressed sample a significant improvement in the spontaneous polarization has been observed with a value of $P_{max} = 1.3$ μC/cm^2. Similarly a small increase in the remanent polarization $P_r = 0.54$ μC/cm^2 and coercive field $E_c = 5.49$ kV/cm were also observed. The obtained polarization value was higher in the BFO-MF samples than that observed by Mahesh Kumar et al. [4]. In $BiFeO_3$ spontaneous polarization mainly comes from the hybridization between $6s^2$ lone electron pair of Bi^{3+} ion and the 6p empty orbital of O^{2-} ion, which induces non-centrosymmetric distortion of the electron cloud and results in ferroelectricity. The R3c symmetry also permits the development of spontaneous polarization along [1 1 1], where Bi, Fe, and O are displaced relative to one another along this 3-fold axis. The largest displacements in $BiFeO_3$ are from Bi relative to O, consistent with stereochemically active Bi lone pairs [17].

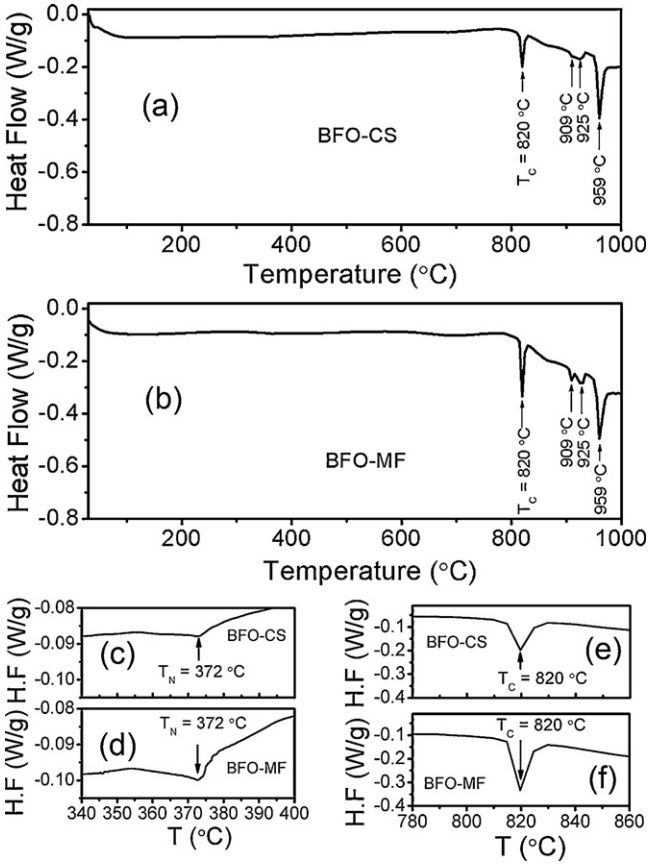

Fig. 4. High temperature DSC curves of (a) BFO-CS and (b) BFO-MF samples. DSC curves showing Neel transition temperature (T_N) for (c) BFO-CS and (d) BFO-MF samples. DSC curves showing ferroelectric curie transition temperature (T_C) for (d) BFO-CS and (e) BFO-MF samples.

According to Wang et al., apart from inducing magnetization that is approximately proportional to a magnetic field H, an applied magnetic field results in a polarization change in the $BiFeO_3$ particles due to the ME effect and that the destruction of a cycloid results in a significant enhancement in the spontaneous polarization [18]. Further the improved polarization values in magnetic field pressed $BiFeO_3$ could also be due to the non-centrosymmetric distortion of Fe electron cloud, by the applied magnetic field during compaction. The application of high electric field was restricted due to higher conductivity of the sample causing large current leakage. The lower resistivity of BFO was due to the formation of Fe^{2+} ions by valence fluctuation created due to oxygen deficiency during the sintering process.

High temperature DSC curves of conventional and in-situ magnetic field pressed BFO ceramic were shown in Fig. 4(a) and (b). The DSC peaks shown in Fig. 4(c) and (d) exhibits an apparent λ-type, indicating a second order transition. Thus the observed endothermic DSC peaks correspond to the anti-ferromagnetic to paramagnetic transition (T_N) is consistent with the reported T_N values of BFO [19]. Beyond 800 °C four sharp peaks exists around 820 °C, 909 °C, 925 °C and 959 °C for both the samples. The first strong endothermic peak corresponds to the well known ferroelectric to paraelectric transition temperature (or α to β phase transition) [20]. The second transition corresponds to the decomposition of minor secondary phases (i.e., Bi_2Fe_4O). The third transition is related to β to γ phase transition (ferroelastic transition) [21]. The last strong endothermic peak corresponds to the decomposition temperatures of BFO. On close observation as shown in Fig. 4(c)–(f), a significant change in the heat flow and enthalpy was observed in the magnetic field pressed samples at their Neel and ferro-paraelectric transitions. A change in enthalpy of $\Delta H = 3.453$ J/g and $\Delta H = 5.551$ J/g for BFO-CS and BFO-MF samples respectively was observed. This shows that the magnetic field applied during pressing has certain impact on the structure of BFO ceramic.

4. Conclusions

The structural, thermal and multiferroic (MF) behaviour of BFO ceramic processed by in-situ magnetic field pressing was investigated. It was observed that magnetic field pressing has significant impact on the structural and multiferroic properties of $BiFeO_3$ ceramic. Since, a small magnetic field of 1 T was used in our present investigation, a large variation in multiferroic properties cannot be observed. However, by applying higher magnetic fields during pressing and controlled sintering under oxygen atmosphere can further improve the MF behaviour of BFO ceramic. Recently, numerous research papers have reported improved multiferroic behaviour by doping rare earth ions (RE) at A-site of $BiFeO_3$ ceramic. Hence in-situ magnetic field pressing can prove to be a promising technique to further improve the multiferroic behaviour of RE-doped BFO ceramics and such studies are in progress.

Acknowledgements

The authors gratefully acknowledge Defence Research and Development Organization (DRDO), India, for their financial support to carry out this work. We express our sincere thanks to Dr. G. Malakondaiah – Director, DMRL for his keen interest in the multiferroic materials. We also thank ARCI, Hyderabad for availing high temperature DSC measurement facilities.

References

[1] S.W. Cheong, M. Mostovoy, Multiferroics: a magnetic twist for ferroelectricity, Nat. Mater. 6 (2007) 13–20.
[2] R. Ramesh, N.A. Spaldin, Multiferroics: progress and prospects in thin films, Nat. Mater. 6 (2007) 21–29.
[3] J.R. Teague, R. Gerson, W.J. James, Dielectric hysteresis in single crystal $BiFeO_3$, Solid State Commun. 8 (1970) 1073–1074.
[4] M. Mahesh Kumar, V.R. Palkar, K. Srinivas, S.V. Suryanarayana, Ferroelectricity in a pure $BiFeO_3$ ceramic, Appl. Phys. Lett. 76 (2000) 2764–2766.
[5] J.K. Kim, S.S. Kim, W.J. Kim, Sol–gel synthesis and properties of multiferroic $BiFeO_3$, Mater. Lett. 59 (2005) 4006–4009.
[6] G.A. Smolenski, I.E. Chupis, Ferroelectromagnets, Sov. Phys. Usp. 25 (1982) 475–493.
[7] M. Mahesh Kumar, A. Srinivas, S.V. Suryanarayana, Structure property relations in $BiFeO_3/BaTiO_3$ solid solutions, J. Appl. Phys. 87 (2000) 855–893.
[8] Y.P. Wang, L. Zhou, M.F. Zhang, X.Y. Chen, J.M. Liu, Z.G. Liu, Room-temperature saturated ferroelectric polarization in $BiFeO_3$ ceramics syn-

thesized by rapid liquid phase sintering, Appl. Phys. Lett. 84 (2004) 1731–1733.
[9] A. Srinivas, T. Karthik, V. Kamaraj, V. Chandrasekeran, Improved magnetoelectricity by uniaxial magnetic field pressed and sintered composites in $BaTiO_3$ (x)–$BaFe_{12}O_{19}$ ($1-x$) system (x = 0.8, 0.6), Mater. Sci. Eng., B 172 (2010) 289–293.
[10] V.M. Goldscmidt, The laws of crystal chemistry, Naturwissenschaften 14 (1926) 477–485.
[11] P.M. Woodward, Octahedral tilting in perovskites. II. Structure stabilizing force, Acta Crystallogr., Sect. B: Struct. Sci. 53 (1997) 44–66.
[12] G.K Willamson, W.H. Hall, X-ray line broadening from filed aluminium and wolfram, Acta Metall. 1 (1953) 22–31.
[13] H.P. Klug, L.E. Alexander, X-ray Diffraction Procedures for Polycrystalline and Amorphous Materials, Wiley, New York, 1974.
[14] D. Lee, M.G. Kim, S. Ryu, H.M. Jang, S.G. Lee, Epitaxially grown La-modified $BiFeO_3$ magnetoferroelectric thin films, Appl. Phys. Lett. 86 (2005) 222903–222905.
[15] B. Ruette, S. Zvyagin, A.P. Pyatakov, A. Bush, J.F. Li, V.I. Belotelov, A.K. Zvezdin, D. Viehland, Magnetic-field-induced phase transition in $BiFeO_3$ observed by high field electron spin resonance: cycloidal to homogeneous spin order, Phys. Rev. B: Condens. Matter Mater. Phys. 69 (2004) 064114–064120.
[16] K. Ueda, H. Tabata, T. Kawai, Coexistence of ferroelectricity and ferromagnetism in $BiFeO_3$–$BaTiO_3$ thin films at room temperature, Appl. Phys. Lett. 75 (1999) 555–557.
[17] J.B. Neaton, C. Ederer, U.V. Waghmare, N.A. Spaldin, K.M. Rabe, First principles study of spontaneous polarization in multiferroic $BiFeO_3$, Phys. Rev. B: Condens. Matter Mater. Phys. 71 (2005) 014113–014120.
[18] N. Wang, J. Cheng, A. Pyatakov, A.K. Zvezdin, J.F. Li, L.E. Cross, D. Viehland, Multiferroic properties of modified $BiFeO_3$–$PbTiO_3$-based ceramics: random field induced release of latent magnetization and polarization, Phys. Rev. B: Condens. Matter Mater. Phys. 72 (2005) 104434–104438.
[19] P. Fischei, M. Polemska, I. Sosnowska, M. Szymanski, Temperature dependence of the crystal and magnetic structures of $BiFeO_3$, J. Phys. C: Solid State Phys. 13 (1980) 1931–1940.
[20] R. Haumont, I.A. Kornev, S. Lisenkov, L. Bellaiche, J. Kreisel, B. Dkhil, Phase stability and structural temperature dependence in powdered multiferroic $BiFeO_3$, Phys. Rev. B. Condens. Matter Mater. Phys. 78 (2008) 134108–134115.
[21] R. Palai, R.S. Katiyar, H. Schmid, P. Tissot, S.J. Clark, J. Robertson, S.A.T. Redfern, G. Catalan, J.F. Scott, β phase and γ-β metal–insulator transition in multiferroic $BiFeO_3$, Phys. Rev. B: Condens. Matter Mater. Phys. 77 (2008) 014110–014120.